RESEARCH

Hydration Model and Evaluation of the Properties of Calcined Hwangtoh Binary Blends

Han-Seung Lee[1] and Xiao-Yong Wang[2]*

Abstract

Calcined hwangtoh is a pozzolanic material that is increasingly being used as a mineral admixture in the concrete industry. This study shows a hydration model for cement–hwangtoh blends and evaluates the various properties of hwangtoh-blended concrete using reaction degrees of binders. First, a kinetic reaction model is proposed for analyzing the pozzolanic reaction of hwangtoh. The reaction of hwangtoh includes three processes: the initial dormant period, boundary reaction process, and diffusion process. The mutual interactions between the binary reactions of cement and hwangtoh are thought to be in line with the items in capillary water and calcium hydroxide. Second, the reaction degrees of cement and hwangtoh are determined based on a blended hydration model. Furthermore, the chemical (chemically combined water and calcium hydroxide contents), mechanical (compressive strength), thermal (hydration heat), and durability aspects (carbonation depth) of hwangtoh-blended concrete are systematically predicted. The results show good agreement with experimental results.

Keywords: hwangtoh, hydration model, blended concrete, strength, carbonation

1 Introduction

Hwangtoh is an environmentally friendly material and belongs to the family of clay. Hwangtoh can purify indoor air by absorption, and it is widely used in hospital buildings for reducing sick building syndrome, including sore throat and headaches. On the other hand, after calcination at about 800 ℃, the phase compositions of hwangtoh are changed, and calcined hwangtoh shows pozzolanic reactivity. The pozzolanic reaction of hwangtoh can increase late-age strength of concrete. Summarily, calcined hwangtoh is increasingly used in the cement and concrete industry because of its unique environmentally friendly characteristics and chemical reactivity (Kim et al. 2017).

Many experimental investigations have been performed on the hydration, mechanical, durability, and thermal properties of hwangtoh-blended concrete. Go et al. (2010, 2009) reported that the optimal temperature for thermal activation of hwangtoh is about 800 ℃, thermally activated hwangtoh shows clear pozzolanic activity, and the hydration heat of hwangtoh-blended concrete is lower than that of control concrete. Koo et al. (2014) found the drying shrinkage and carbonation depth of hwangtoh-blended concrete are higher than that in control concrete, and the flexural failure mode of hwangtoh-blended concrete is similar to that of plain concrete. Koo et al. (2015) presented a comparison with a plain environment, where mice in the hwangtoh-blended environment showed higher food and water intake, higher fertility rate, and healthier offspring. Yang et al. (2014) reported a comparison with Portland cement concrete. The slope of the ascending zone of the stress–strain curve

*Correspondence: wxbrave@kangwon.ac.kr
[2] Department of Architectural Engineering, Kangwon National University, Chuncheon-Si 24341, Korea
Full list of author information is available at the end of the article

of hwangtoh-blended concrete is smaller, and the descending zone is steeper. Lin et al. (2019) found that, compared with plain concrete, hwangtoh-blended concrete shows higher late-age strength because of the secondary reaction of hwangtoh. Kim et al. (2012) showed that, based on microwave heating, alkali-activated natural hwangtoh shows high early-age strength. Kwon et al. (2017) presented that after addition of silica fume, the compressive strength of calcium hydroxide activated hwangtoh significantly improved. Yang et al. (2010) found the mechanical properties of alkali-activated hwangtoh-based concrete were significantly influenced by the water-to-binder ratio, not by the sand-to-aggregate ratio. Using hwangtoh, styrene butadiene latex, and shape-stabilized phase change materials, Yang et al. produced hwangtoh boards for building thermal insulation (Yang et al. 2019).

Some numerical models have been proposed for optimal design and performance evaluation of cement-based materials. Perez-Cortes and Escalante-Garcia (2020) made statistical optimization design of alkaline binders of limestone–metakaolin and determined the optimal combinations using the desirability function approach considering strength and sustainability. Sonebi et al. (2020) made the optimal design of rheological parameters of super sulfated cement grouts and captured the significant trends of the tested parameters using statistical models considering bleeding, permeability, and mechanical properties. Yu et al. (2018) predicted the early-age creep and creep recovery of cement paste using a two-step homogenization method and highlighted the effects of the microstructure evolution and inherent creep of C–S–H on the early-age creep. Zhou et al. (2019) analyzed the development of microstructure of cement pastes using a diffusion-based model and considered the effects of particle size distribution, water/cement ratio, temperature, and the ambient humidity. These studies (Perez-Cortes and Escalante-Garcia 2020; Sonebi et al. 2020; Yu et al. 2018; Zhou et al. 2019) show numerical modeling are effective for material design and predictions of material properties.

Although many experimental studies have been performed on the various qualities of hwangtoh-blended concrete, the theoretical models about hwangtoh-blended concrete are extremely limited. To rationally use hwangtoh in the concrete industry, this research suggested a hydration-based framework that could assess the chemical, mechanical, thermal, and durable qualities of hwangtoh-blended concrete. The blended hydration model correspondingly simulates the hwangtoh reaction and cement hydration. The mutual interactions between the reactions of cement and hwangtoh are thought to be in line with the items in capillary water and calcium hydroxide. In addition, the different qualities are evaluated using reaction amounts of binders and concrete mixtures.

2 Hydration-Based Simulation Framework
2.1 Cement Hydration Model
Wang (2019) and Wang and Lee (2019) proposed a hydration model of Portland cement. The hydration model considers the influences of cement compound compositions, cement fineness, concrete mix ratio, and curing conditions on the rate of cement hydration. The hydration degree of cement α can be determined as $\alpha = \int_0^t \left(\frac{d\alpha}{dt} \right) dt$, where $\frac{d\alpha}{dt}$ is the hydration rate. The detailed equation about $\frac{d\alpha}{dt}$ is available in our former studies (Wang 2019; Wang and Lee 2019). The kinetic processes involved in cement hydration, for example, initial dormant period, boundary reaction process, and diffusion-controlled process, are within the suggested hydration model. The input parameter for the cement hydration model is cement mineral compositions and fineness, concrete mix ratio, and curing conditions. The output parameter of the cement hydration model is the reaction amount of cement versus time. The hydration model views the decrease in the rate of hydration because of the lack of capillary water for concrete, which has a lower water-to-cement ratio. Therefore, the hydration model is applicable for concrete with ordinary strength and high strength. In line with the Portland cement hydration model, Wang (2019) and Wang and Lee (2019) evaluated the strength development, adiabatic temperature rise, carbonation, and chloride ingress of Portland cement concrete.

However, the previous models of Wang (2019) and Wang and Lee (2019) is not valid for hwangtoh-blended concrete because the model does not cover the reaction of hwangtoh. To systematically evaluate hwangtoh-blended concrete, a hydration model that considers the binary reactions of cement and hwangtoh is necessary.

2.2 Hwangtoh Reaction Model
This section shows the kinetic reaction model of hwangtoh. The reaction model was obtained based on experimental studies of kinetic hydration processes of cement–hwangtoh blends and the material properties of hwangtoh. The evolution of the reaction degree of hwangtoh with time can be determined using the kinetic reaction model.

Lin et al. measured the isothermal heat release of hwangtoh-blended paste (Lin et al. 2019). They found the kinetic hydration procedure for cement–hwangtoh blends was comparable with Portland cement. The hydration of cement–hwangtoh blends includes initial dormant period, boundary reaction process, and diffusion process.

Go et al. (2010) reported that hwangtoh is a pozzolanic material that can interact with calcium hydroxide. In cement–hwangtoh blends, the hydration of cement produces calcium hydroxide, and the reaction of hwangtoh consumes calcium hydroxide. The content of remained calcium hydroxide in cement–hwangtoh blends is dependent on both cement hydration and hwangtoh reaction. Moreover, as a pozzolanic material, the reaction of hwangtoh relies upon the quantity of remained calcium hydroxide in cement–hwangtoh blends. In thinking about the kinetic reaction procedure for cement–hwangtoh blends and material signs of hwangtoh, the kinetic reaction equation of hwangtoh can be established as follows:

$$\frac{d\alpha_{HT}}{dt} = \frac{m_{CH}(t)}{P} \frac{3\rho_w}{\nu_{HT}r_{HT0}\rho_{HT}} \frac{1}{(\frac{1}{k_{dHT}} - \frac{r_{HT0}}{D_{eHT}}) + \frac{r_{HT0}}{D_{eHT}}(1-\alpha_{HT})^{\frac{-1}{3}} + \frac{1}{k_{rHT}}(1-\alpha_{HT})^{\frac{-2}{3}}},$$ (1)

$$k_{dHT} = \frac{B_{HT}}{(\alpha_{HT})^{1.5}} + C_{HT} * (\alpha_{HT})^3,$$ (2)

$$D_{eHT} = D_{eHT0} * \ln(\frac{1}{\alpha_{HT}}),$$ (3)

where α_{HT} is the reaction degree of hwangtoh; t is time; $m_{CH}(t)$ is the calcium hydroxide (CH) mass in a unit volume of hydrating cement–hwangtoh blends; P is the mass of hwangtoh in the mixture proportion; ν_{HT} is the stoichiometric ratio of hwangtoh to CH [$\nu_{HT} = 0.87$ (Dunster et al. 1993; Papadakis 1999)]; r_{HT0} is the radius of the hwangtoh particle;ρ_{HT} is the density of the hwangtoh; k_{dHT} is the reaction rate coefficient in the initial dormant period (B_{HT} and C_{HT} are coefficients); D_{eHT0} is the initial diffusion coefficient; and k_{rHT} is the reaction rate coefficient in the boundary reaction process.

Within the model, the quantity of capillary water and CH left within the cement–hwangtoh binary system were adopted as control indicators for reactions of binders. The levels of CH ($m_{CH}(t)$), chemically combined water (W_{cbm}), and capillary water (W_{cap}) in cement–hwangtoh blends during hydration can be established using the following equations:

$$m_{CH}(t) = RCH_{CE} * C_0 * \alpha - \nu_{HT} * \alpha_{HT} * P,$$ (4)

$$W_{cap} = W_0 - 0.4 * C_0 * \alpha - 0.46 * \alpha_{HT} * P,$$ (5)

$$W_{cbm} = \nu * C_0 * \alpha + 0.21 * \alpha_{HT} * P,$$ (6)

where RCH_{CE} is the mass of depleted CH as 1 g of cement hydrate. In Eq. (4), the items $RCH_{CE} * C_0 * \alpha$ and $\nu_{HT} * \alpha_{HT} * P$ consider the formation of CH from cement hydration and the depletion of CH due to the hwangtoh reaction. As shown in Eqs. (5) and (6), when 1 g of hwangtoh reacts, 0.21 g combined water is produced and 0.46 g capillary water is consumed (Dunster et al. 1993; Papadakis 1999; Wang 2014). As proven in Eqs. (4, 5, 6), the evolution of CH, chemically combined water, and capillary water in blended concrete relates to both the hwangtoh reaction and cement hydration.

2.3 Properties Evaluation of Hardening Hwangtoh-Blended Concrete

For cement–hwangtoh blends, the hydration products of binders fill pore spaces and lead to the introduction of compressive strength. However, given a particular binder content, a growing water content lowers the concrete strength. The introduction of concrete compressive strength generally starts after the final setting of concrete. Thinking about the reactions of binders, the pore spaces of concrete, and the beginning duration of strength development, the development of strength of hwangtoh-blended concrete can be established utilizing a straight line equation as follows:

$$f_c(t) = A_1 * \frac{C_0 * \alpha}{W_0} + A_2 * \frac{P * \alpha_{HT}}{W_0} - A_3,$$ (7)

where A_1,A_2, and A_3 are strength coefficients. A_1 and A_2 represent the contribution of cement and hwangtoh on strength development, respectively. For concrete with various mixtures at different curing ages, the values of A_1,A_2, and A_3 are constants. Equation (7) shows the concrete strength does not start at mixing time t$=$0, but it starts after a threshold time (Sun et al. 2019). This is similar to the concept of final setting. Final setting means the concrete has started to harden, and this is the beginning of developing the concrete strength (Xu et al. 2017).

The hydration heat of concrete depends on both the hwangtoh reaction and cement hydration. The total released heat can be expressed as the sum of the hwangtoh reaction and cement hydration as follows:

$$\frac{dQ}{dt} = C_0 * H_C * \frac{d\alpha}{dt} + P * H_{HT} * \frac{d\alpha_{HT}}{dt},$$ (8)

where H_C and H_{HT} are the specific heat generation of the cement and hwangtoh, respectively. H_C can be determined from mineral compositions of cement. The value of H_{HT} was proposed as 330 J/g (Riding et al.

2012; Williams 2016). The term $C_0 * H_C * \frac{d\alpha}{dt}$ considers the heat release from the hydration of cement, and the term $P * H_{HT} * \frac{d\alpha_{HT}}{dt}$ considers the heat release from the hwangtoh reaction.

Because of the hwangtoh reaction and cement hydration, the porosity of the hydrating concrete was reduced since hydration started. Papadakis (2000, 1999) and Maekawa et al. (2009) proposed that the total porosity of hydrating concrete can be determined as

$$\varepsilon = \frac{W_0}{\rho_w} - \frac{W_{cbm}}{\rho_{cbm}}, \tag{9}$$

where ε is concrete porosity, and ρ_{cbm} is the density of chemically combined water ($\rho_{cbm} = 1.25$ g/cm³). The term $\frac{W_{cbm}}{\rho_{cbm}}$ means the volume of chemically combined water. Because combined water W_{cbm} depends on the binary reactions of cement and hwangtoh, concrete porosity is a function of concrete mixtures and the reaction degree of binders.

2.4 Evaluation of Carbonation Depth of Hwangtoh-Blended Concrete

When hwangtoh is used as a partial binder in concrete, the carbonation depth increases. In other words, the carbonation durability may be the controlling factor that determines the service life of hwangtoh-blended concrete in an atmospheric environment. The evaluation of carbonation depth is essential for real applications of hwangtoh in concrete structural elements.

Carbonation resistance relates to both internal factors (concrete material properties) and external factors (exposure conditions). The content of carbonated substances, CO_2 diffusivity, CO_2 concentration, and exposure time will affect the carbonation depth. When the relative humidity in the exposure environment is higher than 55%, carbonation is a diffusion-controlled process. The carbonation depth x_c can be determined as follows (Chen and Gao 2019; Chen et al. 2019; Papadakis 2000):

$$x_c = \sqrt{\frac{2D_C([CO_2]_0/100)t}{0.33CH + 0.214CSH}}, \tag{10}$$

$$D_C = A\left(\frac{\varepsilon - \Delta\varepsilon_C}{\frac{C_0}{\rho_c} + \frac{P}{\rho_{HT}} + \frac{W_0}{\rho_w}}\right)^a \left(1 - \frac{RH}{100}\right)^{2.2}, \tag{11}$$

$$CSH(t) = 2.85(f_{S,C} * C_0 * \alpha + f_{S,P} * P * \alpha_{HT}), \tag{12}$$

where D_C is CO_2 diffusivity in the carbonated zone of concrete, and $[CO_2]_0$ is the CO_2 concentration in the exposure environment; CSH is the mass of calcium silicate hydrate in concrete; and $\Delta\varepsilon_C$ is the porosity

reduction of concrete because of carbonation. $\Delta\varepsilon_C$ can be calculated based on the change of solid volume between reactants and products(Papadakis 2000); *RH* is the relative humidity of the exposure environment. *A* and *a* are parameters of carbonation and can be regressed based on measurement results of carbonation depths. The influence of environmental temperature on CO_2 diffusion can be described using the Arrhenius law (Papadakis 2000, 1999).

Equation 12 shows the calculation of CSH. $f_{S,C}$ and $f_{S,P}$ denote the mass percentages of SiO_2 in cement and hwangtoh, respectively. For hwangtoh-blended concrete, both the hwangtoh reaction and cement hydration produce CSH (Riding et al. 2012; Williams 2016; Xu et al. 2017). In Eq. 12, the terms $f_{S,C} * C_0 * \alpha$ and $f_{S,P} * P * \alpha_{HT}$ mean the formation of CSH from the hwangtoh reaction and cement hydration, respectively. The coefficient 2.85 is the molar weight ratio of CSH to SiO_2 in CSH (Papadakis 1999, 2000).

In line with the suggested hydration model, the quantity of CH and CSH and the extent of porosity could be acquired as connected results throughout the hydration duration of cement–hwangtoh blends. In addition, the carbonation depth could be predicted by utilizing Eqs. 10, 11, and 12.

2.5 Summary of Simulation Framework

Figure 1 shows a flowchart of the simulation. First, based on the blended hydration model and concrete mixtures, the reaction degree of binders can be calculated. Furthermore, combined water, CH, and CSH contents can be
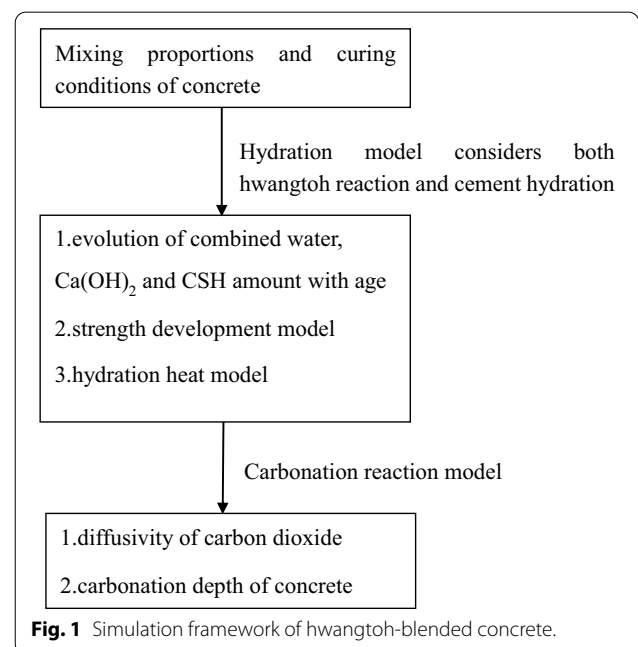
Fig. 1 Simulation framework of hwangtoh-blended concrete.

determined using the reaction degree of binders and concrete mix ratios. The development of strength and hydration heat can be evaluated considering both the hwangtoh reaction and cement hydration. Second, CO_2 diffusivity can be determined based on concrete porosity and environmental conditions. Moreover, carbonation depth can be calculated considering the contents of carbonated substances, CO_2 diffusivity, and CO_2 concentration in the exposure environment. Summarily, the reaction degrees of cement and hwangtoh are key factors for evaluating the various properties of hardening and hardened hwangtoh-blended concrete.

3 Verification of the Proposed Model

As shown in Sect. 2, the proposed model can evaluate various properties of hwangtoh-blended concrete. To verify the proposed model, multiple checks were performed, such as chemical (experimental tests of combined water and CH), mechanical (compressive strength test), thermal (hydration heat), and durability aspects (carbonation depth test). Through these systematic verifications, the validations of the proposed model are shown.

3.1 Evaluation of the Properties of Hardening Concrete

Experimental results in our previous study (Lin et al. 2019) were used to verify the evaluation of the properties of hardening concrete. In our previous studies, the property development of hwangtoh-blended paste with various water-to-binder ratios (W/B 0.5 and 0.2) and hwangtoh replacement ratios (0, 10%, and 20%) was measured. The specimens with a W/B 0.5 represent concrete with ordinary strength, and the specimens with a W/B 0.2 represent ultra-high-performance concrete. Table 1 shows chemical compositions of hwangtoh and cement. Figure 2 shows XRD pattern of calcined hwangtoh, which contains quartz, feldspar, and a small amount of illite. The paste specimens are sealed cured until the aging tests. At the curing ages of 3, 7, and 28 days, the contents of combined water and CH were measured using thermogravimetric analysis, and the strengths of specimens were measured using a compression machine. The isothermal heat evolution was measured in the early 3-day period using TAM-air.

The temperature range of thermogravimetric analysis (TGA) tests was between room temperature and 1050℃. Nitrogen was continuously supplied throughout the test. As shown in Fig. 3a, b (TGA results at the ages of 28 days), there
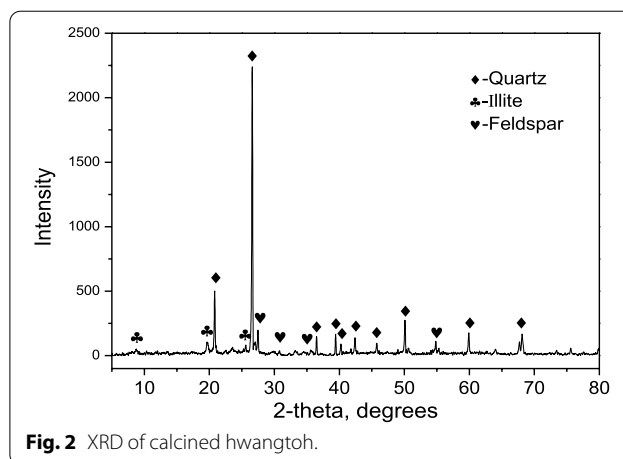

Fig. 2 XRD of calcined hwangtoh.

are three peaks of the differential thermal analysis (DTA) curve. The first peak occurs at about 160 ℃, which corresponds to the dehydroxylation of CSH and AFm (Weerdt et al. 2011). The second peak occurs at about 450 ℃, which corresponds to the decomposition of calcium hydroxide (Weerdt et al. 2011). The third peak occurs at about 700 ℃, which corresponds to the decarbonation of calcite (Weerdt et al. 2011). There are several sources of calcite, such as the limestone powder in cement or the carbonation of specimens while preparing the specimens of TGA (Weerdt et al. 2011). In Korea, the Portland cement contains a small amount (3%-5%) limestone powder (Jeong et al. 2020; Additional file 1: Figures S1, TGA of cement), which is the main reason of the decarbonation peak at 700℃ (Additional file 1: Figures S2 the decarbonation peak of cement and paste). As proposed by De Weerdt et al. (2011), for the specimen with limestone powder, to mitigate the influence of decarbonation stage, non-evaporable water (H) and calcium hydroxide (CH) were calculated at 105–550 ℃ and 400–550 ℃, respectively. The contents of CH can be determined as follows (Weerdt et al. 2011):

$$CH = (W_{400} - W_{550})/W_{550} * (74/18), \qquad (13)$$

where W_{400} and W_{550} are the weights at 400 and 550 ℃, respectively. The item (74/18) means the molar weight ratio of CH to water. The content of non-evaporable water (H) can be determined as follows (Weerdt et al. 2011):

$$H = (W_{105} - W_{550})/W_{550}, \qquad (14)$$

where W_{105} is the weight at 105 ℃.

Table 1 Chemical compositions (%) of cement and hwangtoh.

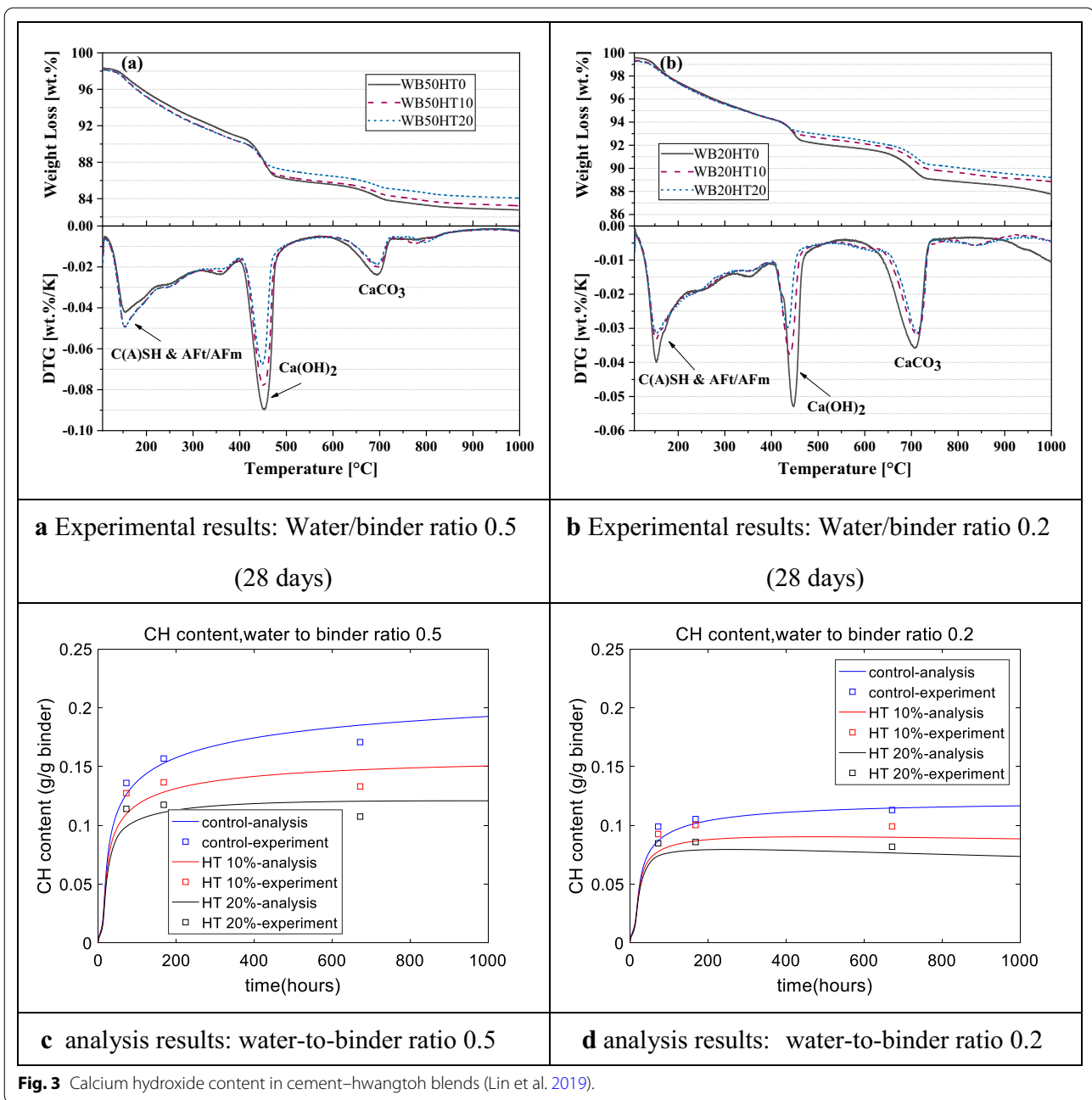|	CaO	SiO$_2$	Al$_2$O$_3$	MgO	Fe$_2$O$_3$	K$_2$O	Na$_2$O	TiO$_2$	SO$_3$	P$_2$O$_5$	ZnO	LOI
Cement	61.30	21.15	5.63	2.34	2.44	1.00	0.44	0.21	2.28	0.09	0.11	3.00
Hwangtoh	0.16	63.9	24.4	0.67	6.13	3.06	–	0.78	–	0.09	–	0.83

Fig. 3 Calcium hydroxide content in cement–hwangtoh blends (Lin et al. 2019).

For hwangtoh-blended concrete, the hwangtoh reaction and cement hydration occurred concurrently. Cement hydration generated CH, and reaction of hwangtoh consumed CH. The generation of CH from cement hydration can be determined based on the cement hydration model. Moreover, the consumption of CH can indicate the reaction degree of hwangtoh. Using the measurement results of CH of cement–hwangtoh blends, the coefficients of the reaction model of hwangtoh are determined and shown

in Table 2. These coefficients do not change with W/B or hwangtoh substitution ratios.

The calculation results of CH are shown in Fig. 3c, d. For plain paste without hwangtoh, the content of

Table 2 Reaction coefficients of hwangtoh.

B_{HT}(cm/h)	C_{HT}(cm/h)	k_{rHT}(cm/h)	D_{eHT0}(cm²/h)
2.67e−11	0.52	7.22e−7	7.06e−13

CH kept increasing at all the ages. In early age, the CH content increased rapidly. At late age, diffusion was the mechanism that controlled cement hydration, and the CH content increased slowly. On the other hand, for cement–hwangtoh-blended paste, the content of CH was less than plain paste. This is because of the reduction of the cement content and the consumption of CH from the hwangtoh reaction. Especially, at the late age, the content of CH decreased due to the proceeding of the hwangtoh reaction (Han and Yan 2015; Han et al. 2017).

Figure 4 shows the reaction degree of binders such as cement or hwangtoh. As shown in Fig. 4a, for the specimen with W/B 0.5, when hwangtoh replaced partial cement, the water-to-cement ratio increased; hence,

the hydration degree of cement increased. This is called the dilution effect of hwangtoh addition. On the other hand, Fig. 4b shows the reaction degree of cement for the specimen with W/B 0.2. From Fig. 4a, b, it can be seen that the dilution effect became obvious with the decreasing water-to-binder ratios. In addition, Fig. 4c presents the reaction level of hwangtoh for various mixtures. It can be seen that as W/B decreased, the reaction level of hwangtoh decreased. This was due to the limitations of available filling space for hydration products. As the hwangtoh replacement ratio increased, the reaction level of hwangtoh also decreased. This was due to the reduction of alkali activation of CH. Compared to the hydration degree of cement (shown in Fig. 4a,

a reaction degree of cement: water-to-binder ratio 0.5

b reaction degree of cement: water-to-binder ratio 0.2

c reaction degree of hwangtoh

Fig. 4 Reaction degree of cement and hwangtoh.
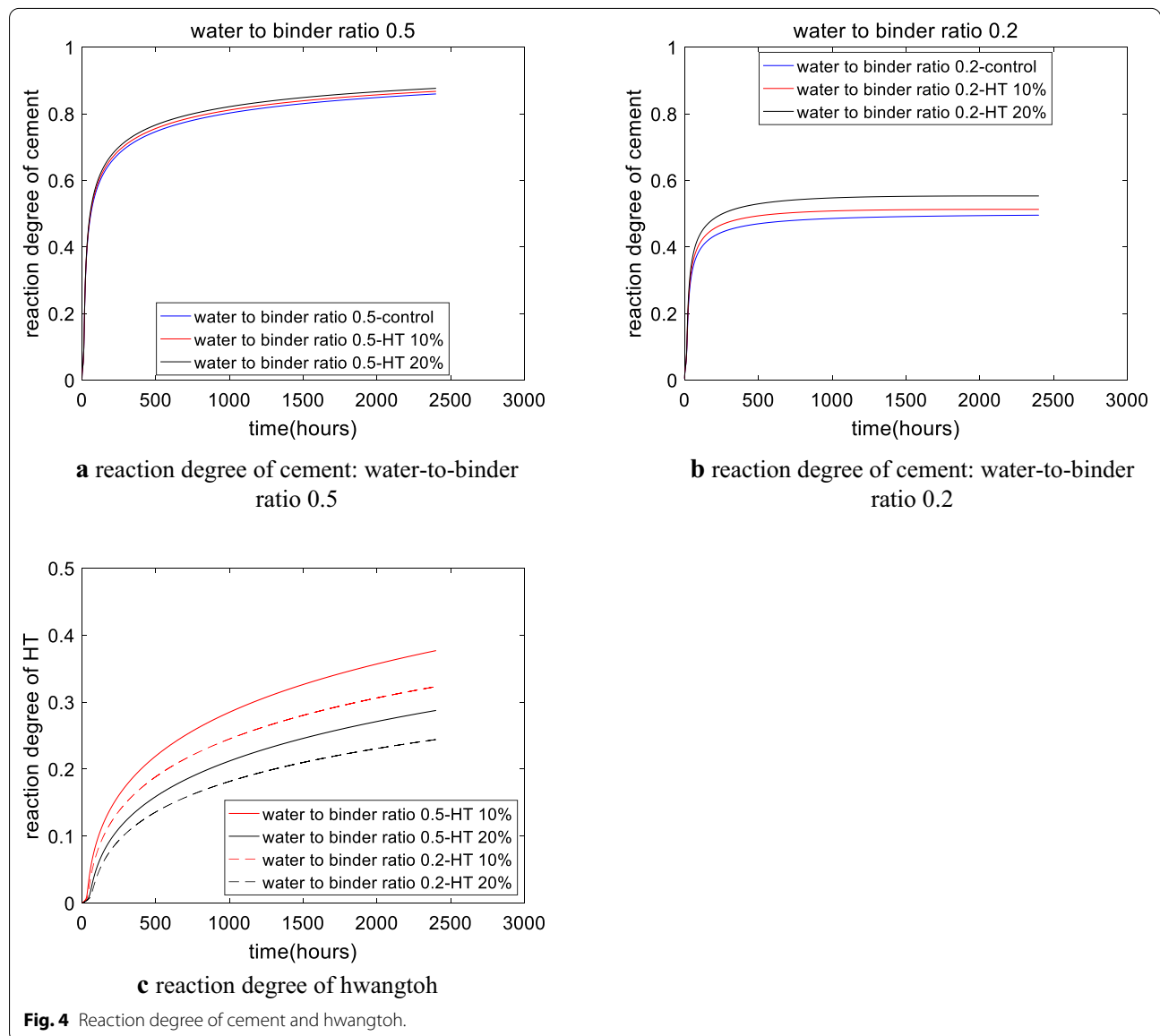
b), the reaction degree of hwangtoh was much lower (shown in Fig. 4c) (Glosser et al. 2019).
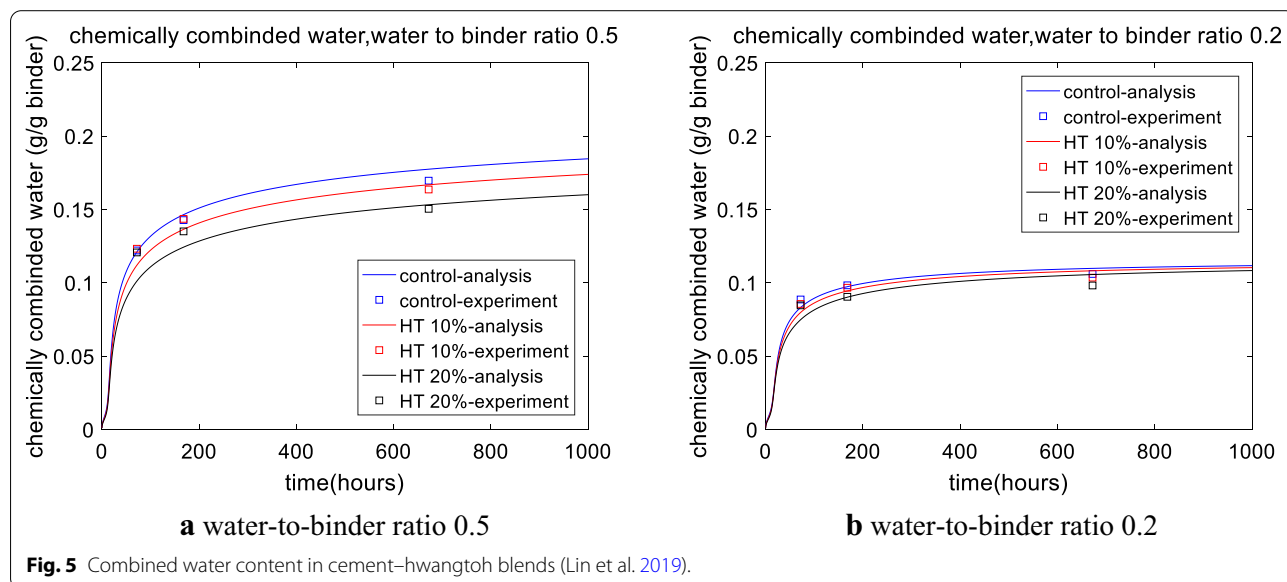
Reaction degrees of cement and hwangtoh are fundamental parameters for evaluating properties of hwangtoh-blended concrete. Based on Eq. (6), the combined water can be determined. As shown in Fig. 5a, when hwangtoh replaced partial cement, the content of combined water decreased. This is because the reactivity of hwangtoh is low compared to cement. As shown in Fig. 5b, as W/B reduced, the content of combined water decreased. This tendency agrees with the trend of the reaction level of binders (Castellano et al. 2016; Riding et al. 2012).

The hydration heat of cement–hwangtoh blends can be evaluated based on the reaction levels of binders. Figure 6 shows the calculation results of hydration heat. In the first 5 h, cement hydration was in the dormant period, and the hydration heat slowly increased. After the initial dormant period, because the boundary reaction process controls hydration, the hydration heat rapidly increased. On the other hand, after the addition of hwangtoh, the hydration heat decreased. This is because the reactivity of hwangtoh is low compared to cement (Lin et al. 2019).

Equation (7) is a linear equation that can evaluate the strength development of hardening concrete. Using the experiment results of specimen strengths, the coefficients A_1, A_2, and A_3 of Eq. (7) were determined to be 58.74, 109.15, and 33.57, respectively. These coefficients did not change with specimen mixtures or curing ages. The prediction results are shown in Fig. 7. First, for the plain specimen, the strength rapidly increased at an early age. At the late age, the increment of strength was not obvious and the strength curve showed a plateau, while for the hwangtoh-blended specimen, at the late age, the

increment of strength was much more obvious than that of the plain specimen. This is due to the slow reaction of hwangtoh that can contribute to the strength development of concrete (Li et al. 2017; Shao et al. 2019). Second, as the W/B decreased from 0.5 to 0.2, the intercept of the strength curve on the x-axis (starting time of strength) decreased. This means the specimen with a lower W/B ratio can develop strength much faster than the specimen with a higher W/B ratio (Han and Yan 2015; Han et al. 2017; Sun et al. 2019). Third, as shown in Fig. 7g, the prediction results showed agreement with measurement results. The correlation coefficient between measurement and evaluation results is 0.993, which proves the validity of proposed strength model. In addition, the proposed strength model is verified using experimental data from another source. Lin et al. (2020) measured the strength development of blended paste with 45% hwangtoh as the binder. The water/binder ratio of paste was 0.5. At the ages of 1, 3, 7, and 28 days, the compressive strength was measured. Using the strength analysis model, the strengths of plain paste and hwangtoh-blended paste are shown in Fig. 7h. The analysis results show agreement with experimental results. Because the reaction of hwangtoh is much slower than that of cement, the starting time of strength of hwangtoh-blended paste is retarded compared with plain paste. Moreover, the 28-day strength of high-volume hwangtoh-blended paste is much lower than that of control paste.

The strength activity index is defined as the ratio of the strength of the hwangtoh–cement blends to the strength of the plain specimen at each specific curing time (Maekawa et al. 2009). At the curing age 28 days, when water/binder is 0.5, the strength activity index for

Fig. 5 Combined water content in cement–hwangtoh blends (Lin et al. 2019).

Fig. 6 Heat of hydration of cement–hwangtoh blends (water-to-binder ratio 0.5) (Lin et al. 2019).
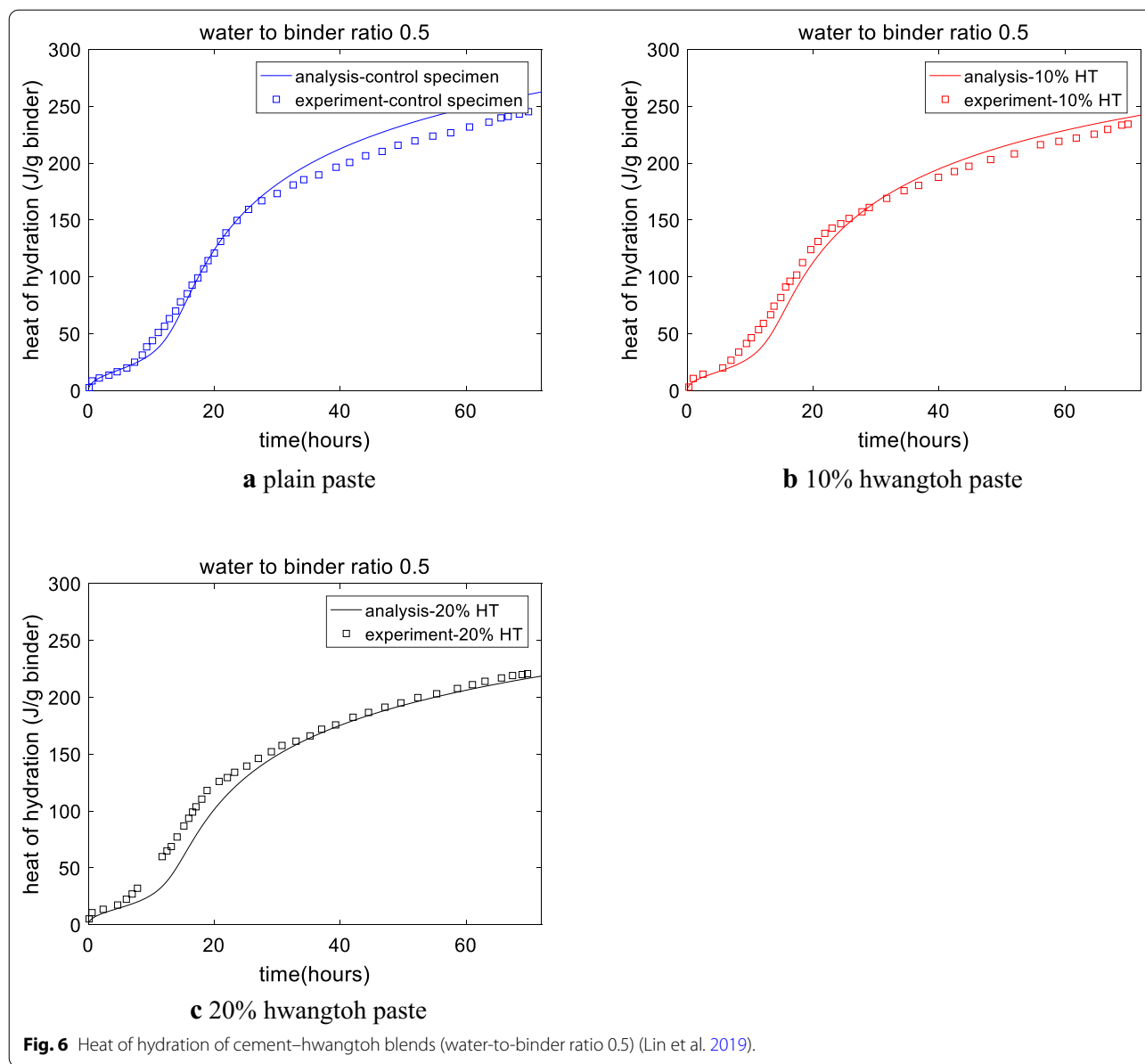
10% hwangtoh and 20% hwangtoh specimen are 1.17 and 1.13, respectively, while when water/binder is 0.2, the strength activity index for 10% hwangtoh and 20% hwangtoh specimen are 1.09 and 1.06, respectively. Summarily, the strength activity index of hwangtoh is dependent on water/binder ratio, hwangtoh replacement levels, and curing ages.

Besides the experimental results of our previous study (Lin et al. 2019), experimental results from Go et al. (2010) are used to verify the proposed hydration model.

Go et al. (2010) made thermal analysis of hydrated plain paste and 20% hwangtoh-blended paste at the ages of 14 days and 28 days. The water/binder ratio of paste specimens was 0.6. The temperature of thermal analysis ranges from 25℃ to 950℃. Based on the experimental results of thermal analysis, the content of calcium hydroxide for the unit mass of binder can be determined. Figure 8 shows the comparisons between calculation results and experimental results of calcium hydroxide contents (Go et al. 2010). The calculation results show
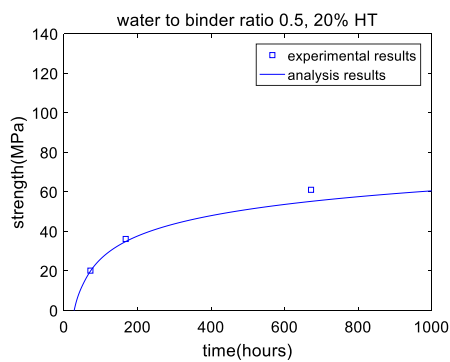
(See figure on next page.)
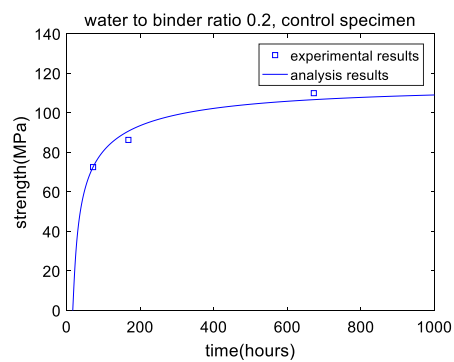**Fig. 7** Strength development of cement–hwangtoh blends (Lin et al. 2019).
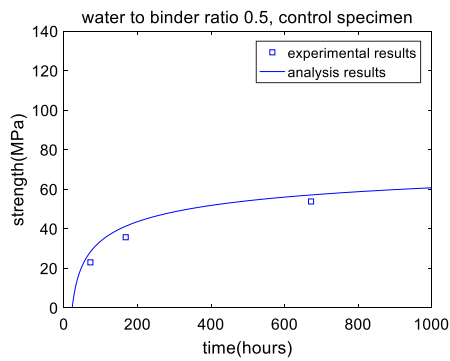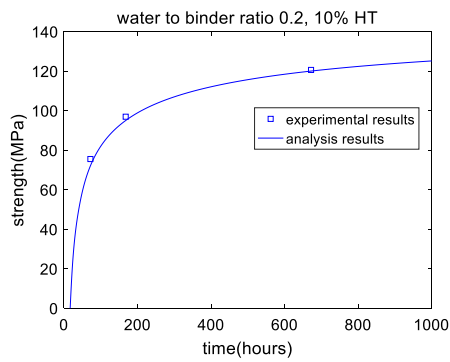
a w/b 0.5 plain paste
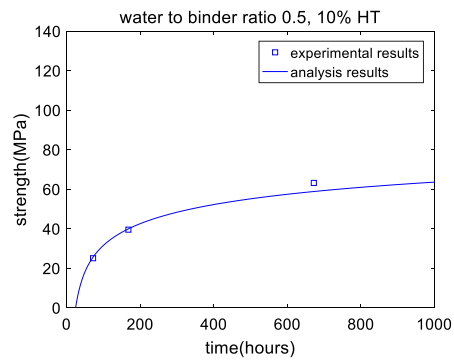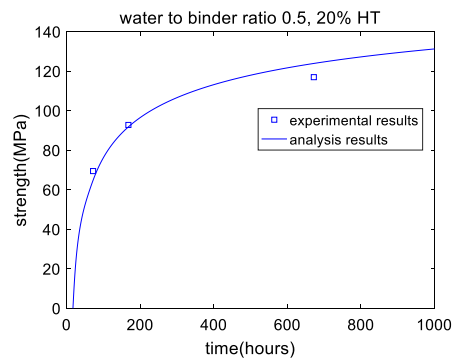
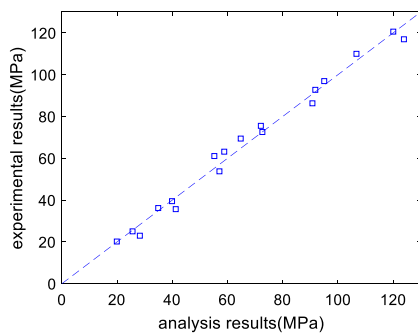**b** w/b 0.5, 10% hwangtoh paste

c w/b 0.5, 20% hwangtoh
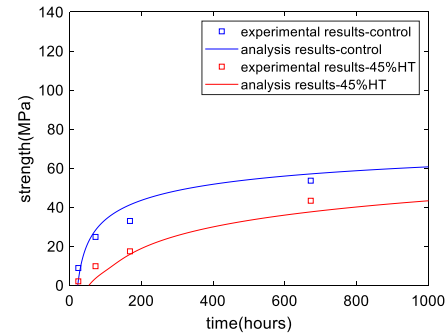
d w/b 0.2, plain paste

e w/b 0.2,10% paste

f w/b 0.2, 20% paste

g experimental results versus evaluation results

h experimental results from another source (Lin et al., 2020)

agreement with experimental results. Due to the dilution effect and pozzolanic reaction of hwangtoh, calcium hydroxide content in blended concrete is much lower than plain concrete.
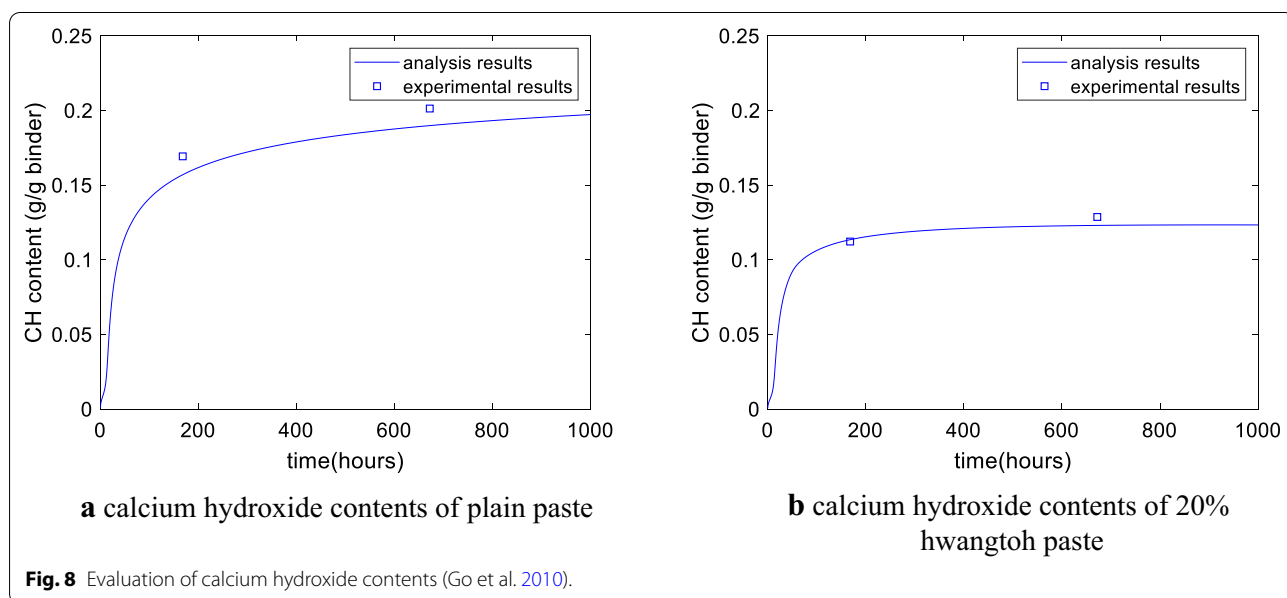
3.2 Evaluation of Carbonation Depth

The experimental study on the carbonation depth of hwangtoh-blended concrete in reference (Koo et al. 2014) was used to verify the proposed model. The W/B of the specimen was 0.55, and the content of binder was 339 kg/m^3. The hwangtoh replacement ratios were 0 and 20%. After 2-month curing, concrete specimens were moved into a CO_2 chamber for accelerated carbonation tests. The CO_2 concentration in the CO_2 chamber was 5%, the relative humidity was 60%, and the temperature was 20 ℃. Carbonation depth was measured at 1, 4, 8, 12, and 25 weeks using the phenolphthalein color change method. Because the hydration of binders essentially stops when relative humidity is less than 80%, further hydration of hwangtoh and cement in the carbonation test period was ignored in this study (Maekawa et al. 2009).
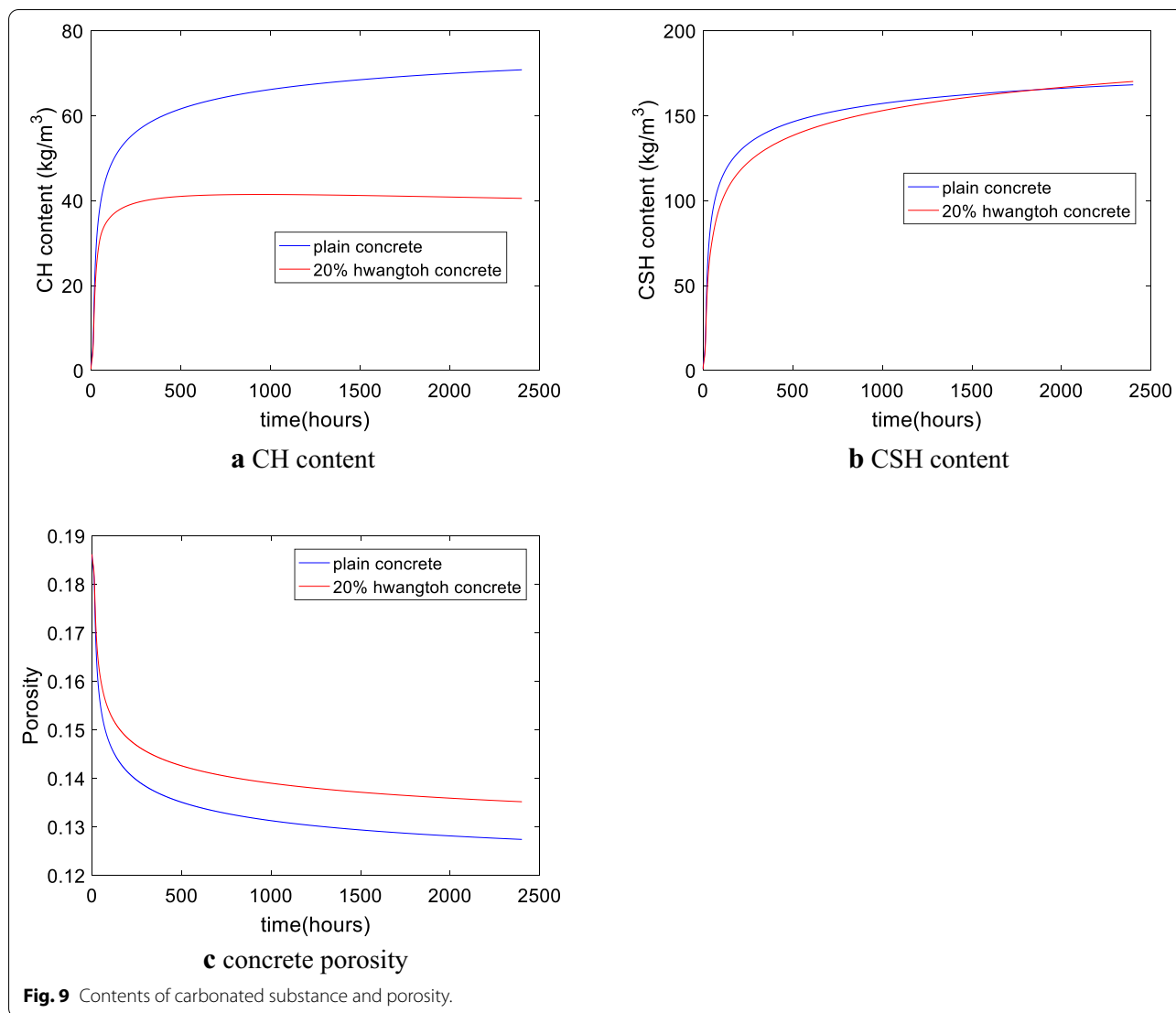
In line with the blended cement hydration model, the items in carbonated substances (CH and CSH) and concrete porosity can be established. First, as proven in Fig. 9a, the CH content of 20% hwangtoh-blended concrete was less than that in plain concrete. Particularly, the CH content decreased in the late ages. Second, as proven in Fig. 9b, at the beginning, the CSH content of hwangtoh-blended concrete was less than that in plain concrete, while at late age, the CSH content of hwangtoh-blended concrete exceeded that of plain concrete. This is because the hwangtoh reaction proceeded, and also the silica

content in hwangtoh is a lot greater than that in cement. Third, as proven in Fig. 9c, the porosity of hwangtoh-blended concrete was greater than that of plain concrete. This trend is comparable with fly ash or slag blended concrete (Han et al. 2017).

According to experimental outcomes of carbonation depth, the coefficients of carbonation model A, along with a are determined as 1.34e−6 and 1.8, correspondingly. The coefficients are comparable with those of Papadakis' study (2000). These coefficients do not change with concrete mixtures and curing conditions. According to the hydration-based carbonation model, the carbonation depth of concrete can be determined. As proven in Fig. 10, the carbonation depth of hwangtoh-blended concrete was a lot greater than that of plain concrete. This really is due to the fact that after adding hwangtoh, the content of CH reduced, and also the porosity and CO_2 diffusivity increased.

Besides the experimental results of Koo et al. (2014), experimental results from Choi et al. (2001) are used to verify the proposed carbonation model. Choi et al. (2001) measured carbonation depths of plain concrete, and 20% hwangtoh-blended concrete. The water/binder ratio of concrete specimens was 0.55, the water content was 179 kg/m^3, and the binder content was 325 kg/m^3. Accelerated carbonation tests started after 28 days of standard curing. The temperature, CO_2 concentration, and relative humidity of acceleration carbonation tests were 20 ℃, 5 and 60%, respectively. After 1-, 2-, 4-, 8-, 10- and 12-week exposure, carbonation depths of concrete were measured using the phenolphthalein indicator method. Figure 11 shows the comparisons between calculation results and experimental results of carbonation depths (Choi et al.

a calcium hydroxide contents of plain paste

b calcium hydroxide contents of 20% hwangtoh paste

Fig. 8 Evaluation of calcium hydroxide contents (Go et al. 2010).

Fig. 9 Contents of carbonated substance and porosity.

2001). The calculation results show general agreement with experimental results. The replacement of partial cement with hwangtoh increases the carbonation depth of concrete.
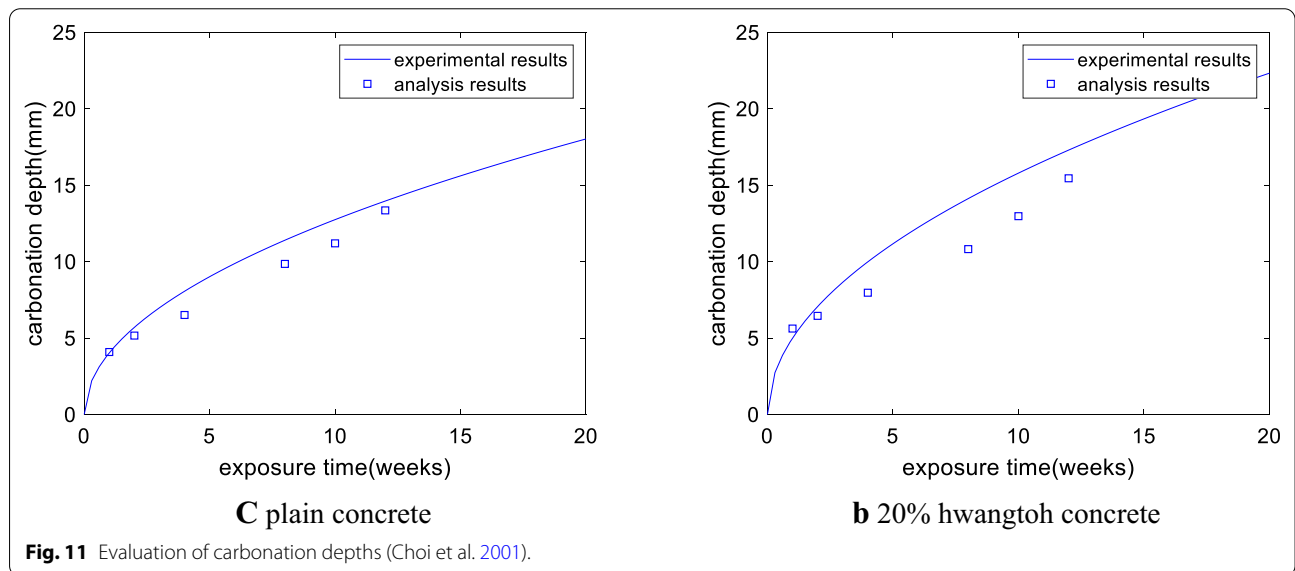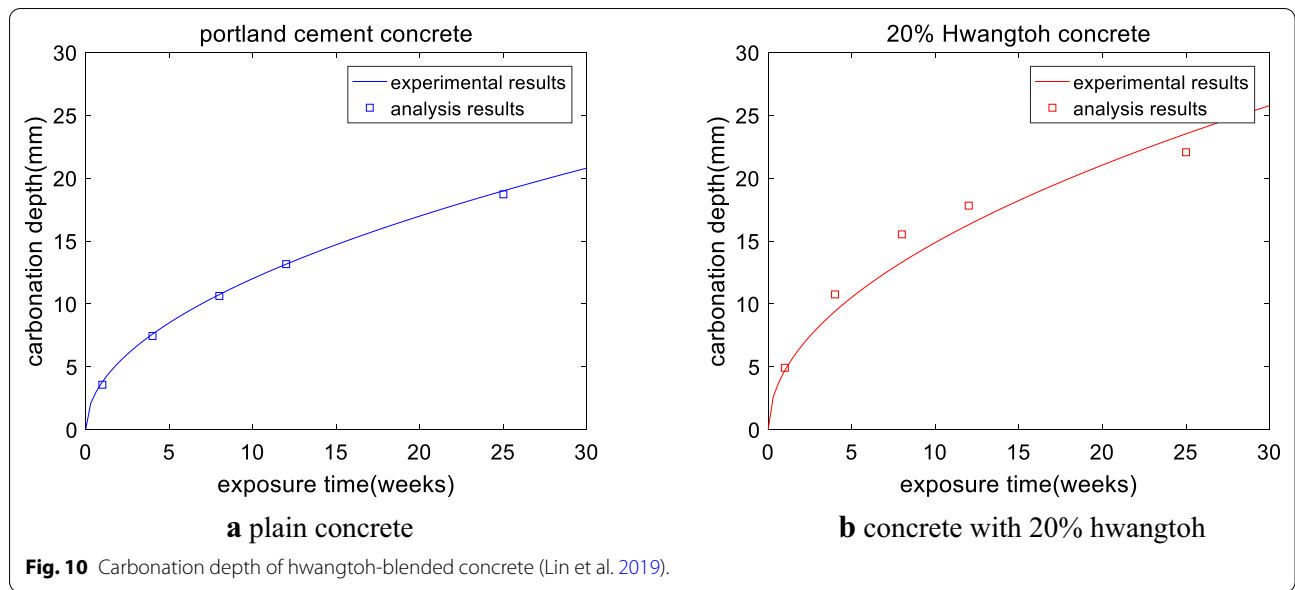
3.3 Discussion

This study shows a hydration-based integrated model for cement–hwangtoh blends. The validation range and the weak points of the proposed model are shown as follows:

First, this study considers several water/binder ratios (0.5, 0.55, 0.6, 0.2) and hwangtoh/binder ratios (10, 20, and 45%). The water/binder ratio 0.2 represents the cases of high-strength concrete and ultra-high-performance concrete, which have a low water/binder ratio and show incomplete hydration due to a shortage of capillary water. The water/binder ratios 0.50, 0.55, and 0.6 represent the cases of ordinary-strength concrete, which have a high water/binder ratio and show sufficient hydration at long-term ages. Hence, the proposed model is valid for both ordinary-strength concrete and high-strength concrete.

Second, hwangtoh is a pozzolanic material and can be used to replace partial cement for concrete production. In construction practices, the replacement levels of hwangtoh are generally lower than 20%. When the replacement level of calcined hwangtoh is lower than 20%, the long-term compressive strength of hwangtoh-blended concrete is comparable or higher than plain concrete. Summarily, the proposed model covers the general replacement levels of hwangtoh in construction practices.

Fig. 10 Carbonation depth of hwangtoh-blended concrete (Lin et al. 2019).

Fig. 11 Evaluation of carbonation depths (Choi et al. 2001).

Third, the limitations of the proposed method are summarized as follows:

(1) The proposed model mainly focuses on concrete with a moderate hwangtoh (less than 20%). For concrete with a high-volume hwangtoh, the reaction of hwangtoh may depend on phase concentration of pore solution and ion movement between inner and outer hydration products (Maekawa et al. 2009; Wang 2014). The hwangtoh reaction model (Eqs. (1), (2), and (3)) may need revisions for considering pore solution and ion movement.

(2) The effects of curing temperature on hwangtoh reaction, strength development, and durability aspect are not covered in this study. Compared with cement, the pozzolanic reaction of hwangtoh may be much more sensitive with temperature (Wang 2014). More experimental study and theoretical modeling should be carried out to clarify the dependence of hwangtoh reaction on temperature.

(3) The proposed model cannot evaluate the phase assemblage of hydrating cement–hwangtoh blends. In the future study, to accurately evaluate the phase assemblage, the proposed kinetic model should

combine with a thermodynamic program, such as Gibbs Energy Minimization (GEM) program (Lothenbach et al. 2019). Moreover, the durability aspects, such as carbonation and chloride, may be evaluated based on phase assemblage of concrete.

4 Conclusions

This research shows an integrated model that simulates the binary hydration of cement–hwangtoh blends and assesses the various properties of cement–hwangtoh blends.

First, a kinetic model was suggested for the hwangtoh reaction. The reaction of hwangtoh was segmented into three stages: the initial dormant period, boundary reaction process, and diffusion process. The suggested model views the dependence of hwangtoh reaction on the CH content. The interaction between the hwangtoh reaction and cement hydration was clarified through CH and capillary water content.

Second, the coefficients of the hwangtoh reaction model were determined in line with the experimental outcomes of CH content of cement–hwangtoh blends. The coefficients of the reaction model are constants for a number of concrete mixtures. The reaction amounts of cement and hwangtoh were determined using blended hydration model. In addition, the combination of water and hydration heat was determined in light of the contributions of hwangtoh reaction and cement hydration.

Third, a hydration-based straight line equation was suggested for evaluating the growing strength of hwangtoh-blended concrete. The coefficients of the strength development model are constants for a number of concrete mixtures. The correlation coefficient between the evaluation and experimental results was 0.993, which proves the suggested strength model applies for ordinary-strength concrete and ultra-high-strength concrete that contains hwangtoh.

Fourth, the contents of carbonated substances and porosity were determined from the hydration model. The CO_2 diffusivity was determined considering the concrete porosity and the relative humidity of the exposure environment. Moreover, the carbonation depth was determined based on a diffusion-controlled equation. The coefficient of the carbonation model did not change for various concrete mixtures. The carbonation model can reflect the increase of carbonation depth due to hwangtoh additions.

Fifth, in a further study, a revised hydration model should be proposed to consider the phase concentration of pore solution, ion movement between inner and outer reaction products, and different curing temperatures.

Moreover, the combination of the proposed kinetic model with a thermodynamic program should be carried out for evaluating the phase assemblage and durability aspects of concrete.

Supplementary Information

The online version contains supplementary material available at https://doi.org/10.1186/s40069-020-00438-5.

Additional file 1: Figure S1. TGA of cement. **Figure S2.** The decarbonation peak of cement and paste.

Authors' information
Han-Seung Lee is a full professor in the Department of architectural engineering at Hanyang University, Korea.

Xiao-Yong Wang is an associate professor in the Department of architectural engineering and Department of Integrated Energy and Infra System at Kangwon National University, Korea.

Author details
[1] Department of Architectural Engineering, Hanyang University, Ansan-Si 15588, Korea. [2] Department of Architectural Engineering, Kangwon National University, Chuncheon-Si 24341, Korea.

References

Castellano, C. C., Bonavetti, V. L., Donza, H. A., & Irassar, E. F. (2016). The effect of w/b and temperature on the hydration and strength of blast furnace slag cements. *Construction and Building Materials, 111,* 679–688.

Chen, T., & Gao, X. (2019). Effect of carbonation curing regime on strength and microstructure of Portland cement paste. *J CO2 Util, 34,* 74–86.

Chen, T., Gao, X., & Qin, L. (2019). Mathematical modeling of accelerated carbonation curing of Portland cement paste at early age. *Cement and Concrete Research, 120,* 187–197.

Choi, H.-Y., Choi, S.-W., Lee, K.-W., Hwang, H.-Z., Kim, M.-H. (2001). An experimental study on the carbonation and resistance to sulfate attack of concrete with hwangtoh admixture, Proceedings of the Architectural

Institute of Korea-Structure & Construction. Architectural Institute of Korea, 21, pp. 353–356.

Dunster, A., Parsonage, J., & Thomas, M. (1993). The pozzolanic reaction of metakaolinite and its effects on Portland cement hydration. *Journal of materials science, 28,* 1345–1350.

Glosser, D., Choudhary, A., Isgor, O., & Weiss, W. (2019). Investigation of reactivity of fly ash and its effect on mixture properties. *ACI Materials Journal, 116,* 193–200.

Go, S., Chung, C., Struble, L., & Lee, H. (2010). Pozzolanic activity of Hwangtoh clay. *Construction and Building Materials, 24,* 2638–2645.

Go, S., Lee, H., Lee, J., Kim, J., & Chung, C. (2009). Experimental investigation of mortars using activated Hwangtoh. *Construction and Building Materials, 23,* 1438–1445.

Han, F., & Yan, P. (2015). Hydration characteristics of slag-blended cement at different temperatures. *Journal of Sustainable Cement-Based Materials, 4,* 34–43.

Han, F., Zhang, Z., & Liu, J. (2017). Effect of water-to-binder ratio on the hydration kinetics of composite binder containing slag or fly ash. *Journal of Thermal Analysis and Calorimetry, 128,* 855–865.

Jeong, Y., Kang, S.-H., Kim, M. O., & Moon, J. (2020). Acceleration of cement hydration from supplementary cementitious materials: Performance comparison between silica fume and hydrophobic silica. *Cement and Concrete Composites, 112,* 103688.

Kim, B., Yi, C., & Kang, K. (2012). Characteristics of alkali-activated natural hwangtoh paste utilizing microwave heating. *Journal of the Korea Institute of Building Construction, 12,* 503–509.

Kim, H., Kim, C., Jeon, J., Lee, S., & Park, C. (2017). Performance evaluation and field application of red clay green roof vegetation blocks for ecological restoration projects. *Sustainability, 9,* 357–372.

Koo, B., Kim, J., Kim, S., & Mun, S. (2014). Material and structural performance evaluations of hwangtoh admixtures and recycled PET fiber-added eco-friendly concrete for CO2 emission reduction. *Materials, 7,* 5959–5981.

Koo, B., Kim, J., Kim, T., & Kim, B. (2015). Material performance and animal clinical studies on performance-optimized hwangtoh mixed mortar and concrete to evaluate their mechanical properties and health benefits. *Materials, 8,* 6257–6276.

Kwon, Y., Kang, S., Hong, S., & Moon, J. (2017). Intensified pozzolanic reaction on kaolinite clay-based mortar. *Applid Science, 7,* 522–534.

Li, C., Zhu, H., Wu, M., Wu, K., & Jiang, Z. (2017). Pozzolanic reaction of fly ash modified by fluidized bed reactor-vapor deposition. *Cement and Concrete Research, 92,* 98–109.

Lin, R.-S., Park, K.-B., Wang, X.-Y., & Zhang, G.-Y. (2020). Increasing the early strength of high-volume Hwangtoh–cement systems using bassanite. *Journal of Building Engineering, 30,* 101317.

Lin, R., Wang, X., Lee, H., & Cho, H. (2019). Hydration and microstructure of cement pastes with calcined hwangtoh clay. *Materials, 12,* 458–478.

Lothenbach, B., Kulik, D. A., Matschei, T., Balonis, M., Baquerizo, L., Dilnesa, B., et al. (2019). Cemdata18: A chemical thermodynamic database for hydrated Portland cements and alkali-activated materials. *Cement and Concrete Research, 115,* 472–506.

Maekawa, K., Ishida, T., & Kishi, T. (2009). *Multi-scale modeling of structural concrete.* London and New York: Taylor & Francis.

Papadakis, V. G. (1999). Effect of fly ash on Portland cement systems Part I. Low-calcium fly ash. *Cement and Concrete Research, 29,* 1727–1736.

Papadakis, V. (2000). Effect of supplementary cementing materials on concrete resistance against carbonation and chloride ingress. *Cement and Concrete Research, 30,* 291–299.

Perez-Cortes, P., & Escalante-Garcia, J. I. (2020). Design and optimization of alkaline binders of limestone-metakaoline A comparison of strength, microstructure and sustainability with Portland cement and geopolymers. *Journal of Cleaner Production, 273,* 123118.

Riding, K., Poole, J., Folliard, K., Juenger, M., & Schindler, A. (2012). Modeling hydration of cementitious systems. *ACI Materials Journal, 109,* 225–250.

Shao, J., Gao, J., Zhao, Y., & Chen, X. (2019). Study on the pozzolanic reaction of clay brick powder in blended cement pastes. *Construction and Building Materials, 213,* 209–215.

Sonebi, M., Abdalqader, A., Fayyad, T., Perrot, A., & Bai, Y. (2020). Optimisation of rheological parameters, induced bleeding, permeability and mechanical properties of supersulfated cement grouts. *Construction and Building Materials, 262,* 120078.

Sun, J., Shen, X., Tan, G., & Tanner, J. (2019). Compressive strength and hydration characteristics of high-volume fly ash concrete prepared from fly ash. *Journal of Thermal Analysis and Calorimetry, 136,* 565–580.

Wang, X.-Y. (2014). Properties prediction of ultra high performance concrete using blended cement hydration model. *Construction and Building Materials, 64,* 1–10.

Wang, X. (2019). Simulation for optimal mixture design of low-CO2 high-volume fly ash concrete considering climate change and CO2 uptake. *Cement and Concrete Composites, 104,* 103408.

Wang, X., & Lee, H. (2019). Effect of global warming on the proportional design of low CO2 slag-blended concrete. *Construction and Building Materials, 225,* 1140–1151.

Weerdt, K. D., Haha, M. B., Saout, G. L., Kjellsen, K. O., Justnes, H., & Lothenbach, B. (2011). Hydration mechanisms of ternary Portland cements containing limestone powder and fly ash. *Cement and Concrete Research, 41,* 279–291.

Williams, A. (2016). *Cracking potential and temperature sensitivity of metakaolin concrete.* USA: University of South Florida.

Xu, G., Tian, Q., Miao, J., & Liu, J. (2017). Early-age hydration and mechanical properties of high volume slag and fly ash concrete at different curing temperatures. *Construction and Building Materials, 149,* 367–377.

Yang, K., Hwang, H., & Lee, S. (2010). Effects of water-binder ratio and fine aggregate-total aggregate ratio on the properties of hwangtoh-based alkali-activated concrete. *Journal of Materials in Civil Engineering, 22,* 887–896.

Yang, K., Mun, J., & Hwang, H. (2014). Stress-strain relationship of Ca(OH)2-activated hwangtoh concrete. *The Scientific World Journal, 2014,* 846805.

Yang, S., Wi, S., Lee, J., Jeon, J., & Kim, S. (2019). Thermal performance evaluation of Hwangtoh board developed with styrene butadiene latex/SSPCM. *Construction and Building Materials, 200,* 310–317.

Yu, P., Duan, Y. H., Chen, E., Tang, S. W., Hanif, A., & Fan, Y. L. (2018). Microstructure-based homogenization method for early-age creep of cement paste. *Construction and Building Materials, 188,* 1193–1206.

Zhou, W., Duan, L., Tang, S. W., Chen, E., & Hanif, A. (2019). Modeling the evolved microstructure of cement pastes governed by diffusion through barrier shells of C–S–H. *Journal of Materials Science, 54,* 4680–4700.

Publisher's Note